

## Orbital ordering in paramagnetic $\text{LaMnO}_3$ and $\text{KCuF}_3$

J. E. Medvedeva,<sup>1,2</sup> M. A. Korotin,<sup>1</sup> V. I. Anisimov,<sup>1</sup> and A. J. Freeman<sup>2</sup>

<sup>1</sup>*Institute of Metal Physics, Yekaterinburg, Russia*

<sup>2</sup>*Department of Physics and Astronomy, Northwestern University, Evanston, Illinois 60208-3112*

(Received 18 January 2002; published 30 April 2002)

*Ab initio* studies of the stability of orbital ordering, its coupling to magnetic structure and its possible origins (electron-phonon and/or electron-electron interactions) are reported for two perovskite systems,  $\text{LaMnO}_3$  and  $\text{KCuF}_3$ . We present an average spin state calculational scheme that allowed us to treat a paramagnetic state and to successfully describe the experimental magnetic or orbital phase diagram of both  $\text{LaMnO}_3$  and  $\text{KCuF}_3$  in crystal structures when the Jahn-Teller distortions are neglected. Hence, we conclude that the orbital ordering in both compounds is purely electronic in origin.

DOI: 10.1103/PhysRevB.65.172413

PACS number(s): 75.20.-g, 71.70.Ej

It is known from earlier studies<sup>1,2</sup> that magnetic ordering is coupled to the orbital ordering (OO)—magnetic interactions depend on the type of occupied orbitals of transition-metal ions. (A very detailed overview on magnetic and OO in cuprates and manganites was given recently by Oleś *et al.*<sup>3</sup>) For example, the OO in  $\text{LaMnO}_3$  reduces the ferromagnetic (FM) contribution from the  $e_g$  orbitals to the inter-layer exchange coupling and is responsible for the stability of the magnetic ground-state structure [which is A-type antiferromagnetic (AFM) below  $T_N=141$  K (Ref. 4)]—as described both experimentally and theoretically on this manganite.<sup>1,4,5</sup> In  $\text{KCuF}_3$ , the OO was obtained in a spin-orbital model<sup>2</sup> as a result of an exchange interaction that correctly describes both orbital and spin alignments simultaneously; thus the spin and orbital degrees of freedom are mutually coupled.

A more complicated picture of the fundamental connection between OO phenomena and forms of the spin alignment follows from experimental measurements that characterize an OO parameter and magnetic interactions in transition-metal oxides. Using the dipole resonant x-ray scattering technique, Murakami *et al.*<sup>6</sup> found a sharp disappearance of OO at much higher temperatures ( $\sim 780$  K) than  $T_N$  in  $\text{LaMnO}_3$ . They suggested a coupling of the spin and orbital degrees of freedom due to the small decrease of the order parameter of the orbital structure above  $T_N$ , even despite the presence of OO in the paramagnetic (PM) phase of  $\text{LaMnO}_3$ . The most striking result was obtained for bilayered  $\text{LaSr}_2\text{Mn}_2\text{O}_7$ ,<sup>7</sup> namely, a competition between the A-type AFM spin ordering with  $T_N \approx 170$  K and the CE-type<sup>4</sup> charge and orbital ordering (COO), which exists between  $T_N$  and COO transition temperature,  $T_{COO} = 210$  K. With decreasing temperature, the development of the COO phase is disrupted by the onset of the A-type AFM ordering at  $T_N$ .

In this paper, we investigate the stability of observed OO's without appealing to magnetic interactions by modeling the PM phase of two manganites,  $\text{LaMnO}_3$  and  $\text{KCuF}_3$ . To this end, we examined all magnetic configurations (MC's) that are mathematically possible in a unit cell of the perovskites that consists of 4 Mn (or Cu) atoms. There are only eight such spin sets as schematically presented in Fig. 2(a). They include the possibility of having FM (labeled "1"), and

C type ("3"), A-type ("6"), and G-type ("7") AFM spin orderings as well as four MC's that have a mathematical meaning, but cannot be realized as an individual magnetically ordered solution. Then, to model a PM state, during the iterations towards self-consistency, we average the orbital occupation matrices (that contain information on the orbital polarization and OO in the unit cell) and potential parameters of all atoms over eight spin-alignment configurations after each iteration. As a result, we have an averaged spin state and can analyze the stability and presence of orbital polarization in such a modeled PM phase. Self-consistency of the averaged spin state calculation (ASSC) is determined by convergence of the averaged total energy, charge densities and orbital occupation matrices.

Typically, the origin of the orbital polarization is believed to be the electron-phonon interaction [the Jahn-Teller (JT) distortion] and the electron-electron interaction. A cooperative JT effect that sets in well above the magnetic transition temperature, stabilizes the particular order of the partly filled  $e_g$  orbitals that are close to orbital degeneracy.<sup>2</sup> Monte Carlo investigations<sup>8</sup> showed a stabilization of the experimental magnetic and OO in  $\text{LaMnO}_3$  only after including lattice distortions. However, a spin-orbital model for insulating undoped  $\text{LaMnO}_3$  derived in Ref. 9 qualitatively explains the observed A-type AFM ordering as stabilized by a purely electronic mechanism.

We investigated two typical pseudocubic perovskites: (i)  $\text{LaMnO}_3$ , in which the strong JT effect breaks the degeneracy of the electronic configuration of  $\text{Mn}^{3+}$  ( $t_{2g}^3 e_g^1$ ) and directly affects the  $e_g$  orbital population. A recent neutron-powder diffraction study, together with thermal analysis,<sup>10</sup> showed that  $\text{LaMnO}_3$  undergoes a structural phase transition at  $T_{JT} = 750$  K above which the OO disappears. To establish the origin of OO in  $\text{LaMnO}_3$ , we performed ASSC's for the high-temperature crystal structure where JT distortions are absent. Since diffraction data<sup>10,11</sup> can be interpreted using two crystal symmetries—double-cubic orthorhombic  $Pbnm$  structure and rhombohedral  $R\bar{3}c$  crystal structure—we did calculations for both. (ii) Another example of a perovskite compound with partly occupied  $e_g$  orbitals resulting in strong JT distortions and strong one-dimensional (1D) AFM interactions is  $\text{KCuF}_3$ . There are two tetragonal crystal types

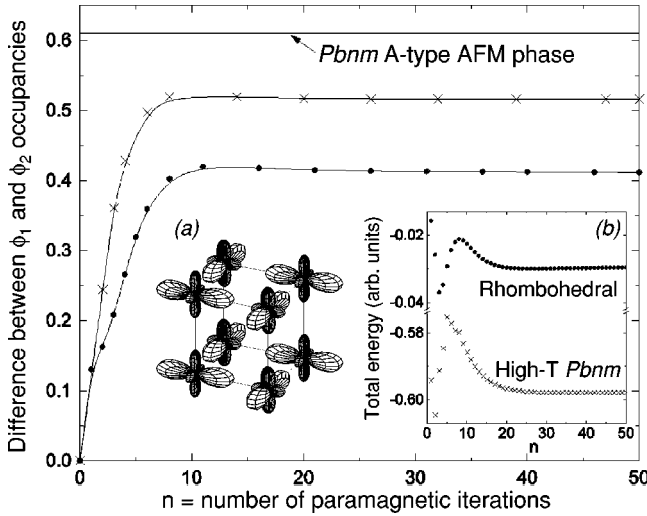


FIG. 1. Dependence of the  $\phi_1 - \phi_2$  difference on the number of PM iterations for the high- $T$  PM phase,  $\delta_{JT}=0.023$  (crosses) and  $R\bar{3}c$  PM phase,  $\delta_{JT}=0.000$  (circles) of  $\text{LaMnO}_3$ . The horizontal line stands for calculated OO of  $Pbmn$  A-type AFM phase,  $\delta_{JT}=0.133$ . In the inset, (a) denotes the angular distribution of the  $e_g$ -electron spin density in the  $Pbmn$  A-type AFM phase of  $\text{LaMnO}_3$  from the LDA+ $U$  calculation and (b) the total energy averaged over all MC's as a function of the number of PM iterations for the two PM phases.

of  $\text{KCuF}_3$ ,<sup>12</sup> which are stable in a wide temperature range, and their A-type AFM ordering temperatures are equal to 20 K and 38 K. It was shown<sup>13</sup> for this compound that the ground state with the lattice distortion and the orbital polarization (and ordering) can be stabilized only by taking into account the Coulomb correlation between  $d$ -shell electrons (LDA+ $U$  approach<sup>14</sup>). We use Coulomb and exchange parameters,  $U=8$  eV and  $J=0.88$  eV for both compounds as those relevant to the 3D transition metal oxides.<sup>14,15</sup>

$\text{LaMnO}_3$ . As the first step, we performed LDA+ $U$  calculations for the experimental A-type AFM phase of  $\text{LaMnO}_3$  with low- $T$   $Pbmn$  structure (where strong JT distortions are present). The self-consistent nondiagonal occupation matrix for the spin density of the  $e_g$  subshell ( $3z^2-r^2$  and  $x^2-y^2$  orbitals) of one particular Mn atom is found to be

$$n_{mm'}^\uparrow, -n_{mm'}^\downarrow = \begin{pmatrix} 0.43 & 0.29 \\ 0.29 & 0.59 \end{pmatrix}.$$

Its diagonalization gives two new  $e_g$  orbitals:  $\phi_1=3x^2-r^2$  ( $3y^2-r^2$  for the second type of Mn atom) with an occupancy of 0.81 and  $\phi_2=z^2-y^2$  ( $z^2-x^2$ ) with an occupancy of 0.20. Since a  $\text{Mn}^{3+}$  ion has formally one electron in the partially filled  $e_g^\uparrow$  subshell and the  $t_{2g}^\uparrow$  subshell is totally filled, we presented the resulting OO by plotting the angular distribution of the  $e_g$  spin density in Fig. 1(a):  $\rho(\theta, \phi) = \sum_{mm'} (n_{mm'}^\uparrow - n_{mm'}^\downarrow) Y_m(\theta, \phi) Y_{m'}(\theta, \phi)$ , where the  $Y_m(\theta, \phi)$  are corresponding spherical harmonics.

The resulting picture of the OO in A-type AFM  $\text{LaMnO}_3$  is in very good agreement with that given by Goodenough<sup>1</sup>

and recently detected using resonant x-ray scattering.<sup>6</sup> Based on this result, we can now move to the case of  $T > T_N$  to investigate the region of the magnetic and orbital phase diagram where the OO exists in the PM phase.<sup>6</sup> To this end, we performed the model ASSC's described above for the high- $T$  (at  $T=798$  K) structure of  $\text{LaMnO}_3$  with experimental lattice parameters.<sup>10</sup> The PM iterations were started from a uniform distribution of  $e_g$  electrons over the  $3z^2-r^2$  and  $x^2-y^2$  orbitals of all Mn atoms. In Fig. 1(b), we plot the “total energy” of the PM state of the high- $T$  structure of  $\text{LaMnO}_3$  (crosses) obtained by averaging the total energies of the eight possible MC's. This total energy curve becomes saturated after the  $\sim 20$ th iteration; hence, we may call this ASSC result self-consistent.

To illustrate the stability of OO in the PM phase and to compare the orbital polarization with that calculated for the experimental A-type AFM phase, we present the OO as a difference between the occupancies of the (“diagonalized”)  $\phi_1$  and  $\phi_2$  orbitals. In Fig. 1, this difference is shown plotted against the number of PM iterations (crosses). We found that starting with equal  $3z^2-r^2$  and  $x^2-y^2$  orbital occupancies (and with a diagonal occupation matrix), the value of the nondiagonal elements of the occupation matrix grows during the ASSC leading to a saturated orbital polarization of the right type [the same obtained for A-type AFM  $\text{LaMnO}_3$ , Fig. 1(a)] around the tenth iteration (Fig. 1). Note that the OO in the PM state is the only stable solution. Forcing different orbital polarizations (ferro-orbitally ordered, etc.) as starting ones for the PM calculation resulted in the type of OO obtained above by changing the corresponding (nondiagonal) orbital occupancy during the iterations towards self-consistency. The horizontal line in Fig. 1 stands for the difference between  $\phi_1$  and  $\phi_2$  orbital occupancies obtained from the usual spin-polarized self-consistent LDA+ $U$  calculation for the A-type AFM phase of  $\text{LaMnO}_3$  in the low- $T$   $Pbmn$  structure. Comparing the orbital polarizations of the PM and AFM phases (Fig. 1), we conclude that the AFM-PM transition in  $\text{LaMnO}_3$  results in a slight decrease of the difference between the  $\phi_1$  and  $\phi_2$  orbital occupancies but does not suppress the OO. This finding agrees with the observed behavior of the OO parameter when  $T$  increases ( $T > T_N$ ).<sup>6</sup>

We need to point out here one essential feature of the ASSC. Since we consider a spin state averaged over eight MC's and, therefore, an average occupation matrix of such a PM state, it is interesting to analyze the deviation of the orbital polarization in each of these MC's from the average value. As seen from Fig. 3(b), where we plot the  $\phi_1$  and  $\phi_2$  orbital occupancy difference for each of the eight MC's after the first (broken line) and fiftieth (solid line) PM iteration, the deviations from the average value become smaller with iterations—they decrease from 36% to 12%, correspondingly. (Further increases of the iteration number do not suppress the deviations.) The variations at the beginning of the ASSC and for the result obtained, c.f., Fig. 2(b), have a close analogy in oscillation behavior, i.e., the location of the  $e_g$  orbital occupancy difference stays higher (lower) with respect to the average value for the same particular MC during the iterations. Hence, one can separate the eight MC's into

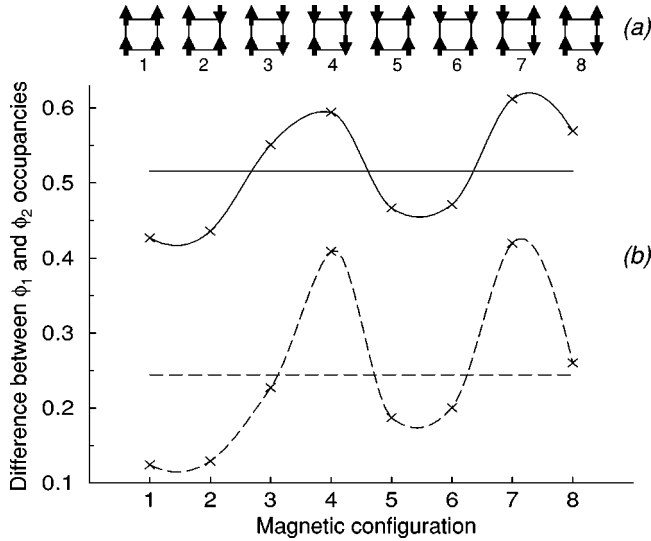


FIG. 2. (a) Schematic illustration of all possible MC's in the unit cell that contains four formula units; only the  $ac$  plane is shown. (b) Deviations of the  $\phi_1 - \phi_2$  difference in each of the MC's considered from the averaged value as a result of ASSC's of the high- $T$  PM phase of  $\text{LaMnO}_3$ . Only the first (broken line) and fiftieth (solid line) iterations are shown.

three groups: the lowest (MC's 1 and 2), the highest (4 and 7) and those close to the average value (3,5,6, and 8).

We analyzed possible reasons for this separation by calculating the number of FM or AFM neighbors aligned to the first Mn [whose spin does not change in all eight MC's, Fig. 2(a)]. First, we found that the behavior of the  $e_g$  orbital occupancy difference curves [Fig. 2(b)] is determined by the spin alignment of nearest neighbors. For both the 1st and 2nd MC's, all six nearest neighbors of the first Mn have the same spin direction, so FM couplings with all nearest neighbors give the smallest  $\phi_1 - \phi_2$  value. By contrast, the largest contributions were obtained from MC's 4 and 7, which have six AFM couplings between the first Mn and its nearest neighbors. The third group of MC's possesses two FM and four AFM couplings (MC 3 and 8), giving almost an exact average value  $\phi_1 - \phi_2$ , and four FM and two AFM couplings (MC 5 and 6), both lying below the average value. (Note here, that it would be sufficient to consider only four MC's: the 1st (which corresponds to the FM phase), the 3rd ( $C$ -type AFM), the 6th ( $A$ -type AFM), and the 7th ( $G$ -type AFM). Averaging over these four MC's underestimates the value averaged over all eight MC's by only 0.7 and 0.1% at the first and 50th PM iteration, respectively.) Thus, we can conclude that the AFM spin alignment seems to be more preferable for OO than the FM one; however, the decrease of the  $\phi_1 - \phi_2$  deviation against the average values (from 47 to 17% for the first and 50th iteration, respectively) in the FM phase also supports the importance of the FM coupling in ASSC.

Let us now discuss some peculiarities in the crystal structure of  $\text{LaMnO}_3$  related to the JT distortions. As found by recent neutron-powder diffraction studies,<sup>10</sup> the JT transition in this perovskite compound occurs at  $T=750$  K. If we define the degree of tetragonal distortion as  $\delta_{JT}=(d_l-d_s)/d_l$

+ $d_s)/2$ , where  $d_l$  and  $d_s$  denote the long and short Mn-O bond distances, then according to the structural data,<sup>10</sup>  $\delta_{JT}$  changes with heating from  $\delta_{JT}=0.133$  for the room- $T$   $Pbmn$  structure to  $\delta_{JT}=0.023$  for the crystal structure at 798 K (which is also orthorhombic  $Pbmn$ , but described as "double-cubic" perovskite<sup>16</sup>). Based on the results obtained above, we may conclude that strong lattice distortions do not influence the OO. However,  $\delta_{JT}$  is not zero in the high- $T$  structure and we have slightly different Mn-O bond distances that break the cubic symmetry, and so the JT effect may still play some role in OO. To check this possibility, we performed ASSC for the rhombohedral  $R\bar{3}c$  structure with lattice parameters taken from.<sup>17</sup> All Mn-O distances are equal in this structure, so  $\delta_{JT}=0.000$ . For this case, the calculated difference between occupancies of the  $\phi_1$  and  $\phi_2$  orbitals against the number of PM iterations is shown in Fig. 1 (circles). This difference is smaller than those obtained for the two orthorhombic structures; nevertheless, we conclude that the OO does not disappear in regular  $\text{MnO}_6$  octahedra, and hence JT distortions are not the origin of the OO in  $\text{LaMnO}_3$ .

$\text{KCuF}_3$ . As shown by Kugel and Khomskii,<sup>2</sup>  $\text{KCuF}_3$  is an example of a system in which the exchange interaction alone results in the correct OO. *Ab initio* LDA+ $U$  investigations<sup>13</sup> confirmed the electronic origin of the ordering: the coupling to the lattice is not a driving force for the orbital (and magnetic) ordering, but the lattice follows the orbital state. Hence, we performed ASSC's for a model structure of  $\text{KCuF}_3$  in which cooperative JT lattice distortions were neglected. We used the tetragonal ( $P4/mmm$ ) crystal structure with  $a=5.855$  Å,  $c=7.846$  Å and the coordinates: K (0, 0.5, 0.45), Cu (0, 0, 0), F1 (0, 0, 0.45), and F2 (0.25, 0.25, 0). In this structure, the  $\text{CuF}_6$  octahedra are slightly compressed along the  $c$  axis: the distance from the Cu atom to the apical F1 atom  $D(\text{Cu-F1})=1.96$  Å, while in the  $ab$  plane  $D(\text{Cu-F2})=2.07$  Å (without the quadrupolar deformation in the  $ab$  plane that is present in the experimental structure).

Since this perovskite compound possesses two energetically equivalent types of OO's characterized by alternation of the  $x^2-z^2$  and  $y^2-z^2$  orbitals,<sup>2,18</sup> we performed four ASSC's that started with different  $e_g$ -electron distributions over Cu  $e_g$  orbitals: the orbital polarizations chosen corresponded to F-type ferro-orbital and A-, C-, or G-type antiferro-orbital alternations of  $x^2-z^2/y^2-z^2$  orbitals (shown in the upper row of OO's in Fig. 3); the C- and G-orbital configurations were observed experimentally.<sup>18</sup> Since a  $\text{Cu}^{2+}$  ion ( $d^9$  configuration) has one hole in the  $e_g$  state, we again represent the OO's by a  $2 \times 2$   $e_g$ -orbital occupation matrix,  $n_{mm'}^\uparrow - n_{mm'}^\downarrow$ . As a start, we used

$$n_{mm'}^\uparrow - n_{mm'}^\downarrow = \begin{pmatrix} 0.53 & \pm 0.28 \\ \pm 0.28 & 0.15 \end{pmatrix},$$

whose diagonalization gives  $x^2-z^2$  ( $y^2-z^2$ ) orbitals.

In contrast to  $\text{LaMnO}_3$ , we found some stable solutions with different OO's in  $\text{KCuF}_3$ . In Fig. 3, we present the total energy of the PM phase for each of the orbital ordered states obtained against the number of PM iterations. The corre-

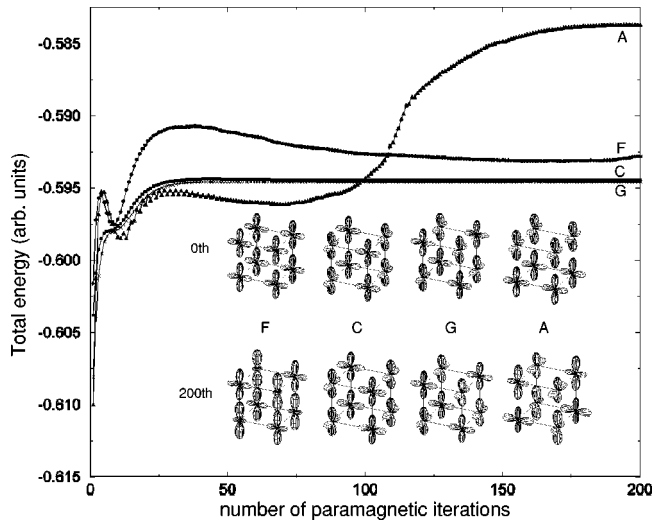


FIG. 3. Total energies of four solutions with different OO's for  $\text{KCuF}_3$  as a function of the number of PM iterations. The corresponding OO (F-type ferro-orbital and A-, C-, or G-type antiferro-orbital orderings) are shown for the zeroth (top row) and the 200th iteration (bottom row).

sponding angular distributions of the  $e_g$  spin density for every solution (at the 200th iteration) are shown (bottom row of OO's in Fig. 3); the antiferro-orbitally ordered state (A) has the highest total energy. Although it seemed to be stabilized with the lowest total energy and with almost fully occupied  $3z^2-r^2$  orbitals at all Cu sites at around the 70th PM

iteration, further PM iterations resulted in a sharp increase of the total energy of this A-type solution, and at the 200th iteration the OO is an alternation of  $3z^2-r^2$  and  $3x^2-r^2/3y^2-r^2$  orbitals. For the calculation, which was started from F-type ferro-orbital ordering, the same  $x^2-y^2$  orbitals at all Cu sites (upper row of Fig. 3) change to almost fully occupied  $3z^2-r^2$  orbitals during the PM iterations (bottom row in Fig. 3).

More preferable in energy are two (almost degenerate) solutions that correspond to G- and C-type OO. Their  $\phi_1$  and  $\phi_2$  orbitals,  $x^2-z^2$  and  $y^2-z^2$ , stagger in the  $ab$  plane, but have ferro- or antiferro-orbital alignments along the  $c$  axis for C or G-type ordering, respectively. This result agrees with previous theoretical and experimental studies on OO in  $\text{KCuF}_3$ .<sup>2,13,18</sup> Thus, from the behavior of the total energy curves of these four solutions, we conclude that PM  $\text{KCuF}_3$  with uniform  $\text{CuF}_6$  octahedra possesses two OO's of the right type.

In summary, the new ASSC scheme presented to treat a PM state successfully described the experimental magnetic and orbital phase diagram of both  $\text{LaMnO}_3$  and  $\text{KCuF}_3$  without inclusion of JT distortions. The OO in the PM phase is found to be the same type as in the AFM phase. A small decrease of the order parameter of the OO upon the AFM-PM transition is in agreement with the observed one. Finally, we conclude that OO in both  $\text{LaMnO}_3$  and  $\text{KCuF}_3$  is of purely electronic origin.

Work supported by the Russian Foundation for Basic Research (Grant No. RFFI-01-02-17063) and the U.S. Department of Energy (Grant No. DE-F602-88ER45372).

- <sup>1</sup>J.B. Goodenough, *Phys. Rev.* **100**, 564 (1955).
- <sup>2</sup>K.I. Kugel and D.I. Khomskii, *Sov. Phys. Usp.* **25**, 231 (1982); *Zh. Éksp. Teor. Fiz.* **64**, 1429 (1973) [*Sov. Phys. JETP* **37**, 725 (1973)].
- <sup>3</sup>A.M. Oleś, M. Cuoco, and N.B. Perkins, in *Lectures on the Physics of Highly Correlated Electron Systems IV*, edited by F. Mancini, AIP Conf. Proc. No. 527 (AIP, Melville, NY, 2000), p. 226-380.
- <sup>4</sup>E.O. Wollan and W.C. Koehler, *Phys. Rev.* **100**, 545 (1955).
- <sup>5</sup>K. Terakura *et al.*, *Mater. Sci. Eng., B* **B63**, 11 (1999).
- <sup>6</sup>Y. Murakami *et al.*, *Phys. Rev. Lett.* **81**, 582 (1998).
- <sup>7</sup>T. Chatterji *et al.*, *Phys. Rev. B* **61**, 570 (2000).
- <sup>8</sup>T. Hotta, S. Yunoki, M. Mayr, and E. Dagotto, *Phys. Rev. B* **60**, R15 009 (1999).
- <sup>9</sup>L.F. Feiner and A.M. Oleś, *Phys. Rev. B* **59**, 3295 (1999).
- <sup>10</sup>J. Rodriguez-Carvajal *et al.*, *Phys. Rev. B* **57**, R3189 (1998).
- <sup>11</sup>Q. Huang *et al.*, *Phys. Rev. B* **55**, 14 987 (1997).
- <sup>12</sup>M.T. Hutchings, E.J. Samuelsen, G. Shirane, and K. Hirakawa, *Phys. Rev.* **188**, 919 (1969); A. Okazaki, *J. Phys. Soc. Jpn.* **26**, 870 (1969); **27**, 518 (1969).
- <sup>13</sup>A.I. Liechtenstein, J. Zaanen, and V.I. Anisimov, *Phys. Rev. B* **52**, R5467 (1995).
- <sup>14</sup>V.I. Anisimov, J. Zaanen, and O.K. Andersen, *Phys. Rev. B* **44**, 943 (1991); V.I. Anisimov, F. Aryasetiawan, and A.I. Liechtenstein, *J. Phys.: Condens. Matter* **9**, 767 (1997).
- <sup>15</sup>S. Satpathy, Z.S. Popovic, and F.R. Vukajlovic, *Phys. Rev. Lett.* **76**, 960 (1996); I. Solovyev, N. Hamada, and K. Terakura, *Phys. Rev. B* **53**, 7158 (1996).
- <sup>16</sup>A. Vegas *et al.*, *Acta Crystallogr., Sect. B: Struct. Sci.* **42**, 167 (1986).
- <sup>17</sup>J.F. Mitchell *et al.*, *Phys. Rev. B* **54**, 6172 (1996).
- <sup>18</sup>K. Hirakawa and Y. Kurogi, *Prog. Theor. Phys.* **46**, 147 (1970).